Fabrication of high-performance SiO_2@p-CuO/n-Si core-shell structure based photosensitive diode for photodetection application

S. Gunasekeran , D. Thangaraju , R. Marnadu ,
J. Chandrasekaran , T. Alshahrani , Mohd Shkir , A. Durairajan ,
M.P.F. Graça , M. Elango

PII: S2468-0230(20)30614-3
DOI: https://doi.org/10.1016/j.surfin.2020.100622
Reference: SURFIN 100622

To appear in: *Surfaces and Interfaces*

Received date: 15 July 2020
Revised date: 23 July 2020
Accepted date: 31 July 2020

Please cite this article as: S. Gunasekeran , D. Thangaraju , R. Marnadu , J. Chandrasekaran , T. Alshahrani , Mohd Shkir , A. Durairajan , M.P.F. Graça , M. Elango , Fabrication of high-performance SiO_2@p-CuO/n-Si core-shell structure based photosensitive diode for photodetection application, *Surfaces and Interfaces* (2020), doi: https://doi.org/10.1016/j.surfin.2020.100622

Fabrication of high-performance SiO_2@p-CuO/n-Si core-shell structure based photosensitive diode for photodetection application

S. Gunasekeran,[a] D. Thangaraju,[b*] R. Marnadu,[c] J. Chandrasekaran,[c] T. Alshahrani,[d] Mohd Shkir,[e] A. Durairajan, [f] M.P.F. Graça,[f] and M. Elango[a*]

[a]*Department of Physics, PSG College of Arts and Science, Coimbatore-641014, Tamil Nadu, India*

[b]*nano-crystal Design and Application Lab (n-DAL), Department of Physics, PSG Institute of Technology and Applied Research, Coimbatore-641062, Tamil Nadu, India*

[c]*Department of Physics, Sri Ramakrishna Mission Vidyalaya College of Arts and Science, Coimbatore 641 020, Tamil Nadu, India*

[d]*Department of Physics, College of Science, Princess Nourah Bint Abdulrahman University, Riyadh, 11671 Saudi Arabia*

[e]*Advanced Functional Materials and Optoelectronic Laboratory (AFMOL), Department of Physics, Faculty of Science, King Khalid University, Abha, 61413, Saudi Arabia*

[f]*I3NAveiro, Department of Physics, University of Aveiro, 3810 193 Aveiro, Portugal*

Corresponding author
**E-mail: dthangaraju@gmail.com (D. Thangaraju)*
Tel: +91 8098768306
**E-mail: elango@psgcas.ac.in (M. Elango)*
Tel: +91 9940709507

Abstract

Core-shell SiO_2@p-CuO semiconductor composite structure-based junction diodes were fabricated by using a metal oxide semiconducting material. The core-shell SiO_2@p-CuO composite structure was successfully fabricated by co-precipitation route. X-ray diffraction (XRD) and Raman spectroscopy is used to inspect the structure & vibrational modes. Field Emission SEM (FE-SEM) was used to analyse the morphology. XRD confirms the existence of monoclinic structure in the pure CuO and SiO_2@p-CuO and Raman studies further establish the formation of a single-phase structure in annealed samples. Crossed nanoflakes-like surface morphology of CuO and formation of core-shell SiO_2@p-CuO structure was verified with FE-SEM micrographs. Fabricated SiO_2@p-CuO/n-Si junction diode shows better photo-response along with a better ideality factor of 3.96 under a light condition than the p-CuO/n-Si. The photosensitivity, responsivity, external quantum efficiency, and detectivity of the developed SiO_2@p-CuO/n-Si diodes is estimated ~ 580471.4%, ~ 259.7 mA/W, ~ 100.7%, 1.715×10^{12} Jones, respectively which are several times larger than the bare p-CuO/n-Si, which are estimated ~ 5320.3%, ~ 230.6 mA/W, ~ 89.4% and 1.561×10^{11} Jones, respectively. The enhanced photodetection properties of SiO_2@p-CuO/n-Si diodes diode proposes it as a mesmerizing aspirant for photodetector application.

Keywords: Copper oxide; Silica; Core-shell; I-V characteristics; Photodiode; photodetector

1. Introduction

Metal oxides semiconducting nanomaterials have received wide attention and attracted to the researchers to fabricate potential devices in optoelectronic fields, particularly in photo detectors, solar cells, sensor, nanomedicine and nanotoxicology modelling applications due to their prominent electrical, optical properties and it exhibit high detectivity and photo response in device performance [1-5]. In recent years, several researchers reported

the fabrication of photodiodes using various metal oxide semiconducting layers such as TiO_2, WO_3, MoO_3, CuO, and V_2O_5 with various preparation methods including green synthesis [6-9].

Among them, copper oxide (CuO) has several advantages such as narrow bandgap (1.2 - 1.9 eV), non-toxic, earth-abundant, ease of synthesis, low thermal emittance, excellent electrical properties, higher carrier concentration [10, 11]. The single-phase monoclinic CuO has extensive attention due to its numeral applications in microelectronic and optoelectronic applications, in particular photo detector, sensor, diode, and solar cell applications [12-14]. The heterojunction diode based on the structure of p-CuO/n-ZnO through the sol-gel routed spin coating method with efficient absorption of UV light by the semiconducting layer was reported by Rajeev et al. [15]. The non-ideal behaviour of diode-based on DC sputtered p-CuO/n-Si was reported by Tombak et al. and electrical nature of green synthesized p-CuO/n-ZnO reported by Sridevi et al. [16, 17]. Zhang et al. reported the p-CuO/n-MoS_2 heterojunction based flexible photo detector developed via magnetron sputtering/CVD and noticed the detectivity of 3.27×10^8 Jones [18]. Hong et al. used solution process to develop CuO/Si nanowire like photodetector and investigated under different wavelengths and the values of responsivity (R), and detectivity (D*) between 0.389 to 0.064 mA/W and 3×10^9 to 7.6×10^9 cm 0.040 to 0.123 A/W [19]. Fu et al. fabricated ZnO/CuO photodetector and noticed the values of P_s and R ~ 120 and 0.272 mA/W [20]. Noothongkaew et al. developed CuO/ZnO UV-photodetector and studied [21]. Very recently Yin et al. reported the development of photodetector based on CuO/Ni@CuO with high performance [22]. Tripathi et al. fabricated the tailored photodetector properties of CuO by tailoring the band gap through varying the morphology and noticed the P_s and D* of $\sim10^3$ and 2.24×10^{11} Jones at 900 nm and 122 and 2.74×10^{10} Jones at 250 nm light wavelengths and the UV-C detector indicates a P_s of 1.8 and D* of 4×10^9 Jones at 250 nm light wavelength [23]. Ji et al.

fabricated the p-CuO nanospheres/n-ZnO nanorods UV-photodetector [24]. Various routes such as spray pyrolysis, CVD, and PLD are followed to fabricate the CuO and related photosensitive layers/photodetectors. The methods described above have limitations such as vacuum circumstance and thickness control of layer [25-35].

Solution-processed thin-film preparation allows coating desired designed nanostructures as a thin-film without destroying its morphology. This method is cost-effective and easy to fabricate the photo sensitive layers [36]. Furthermore, the solution-processed uniform structure enhances the efficiency of the light absorption, and charge carriers are effectively transported by photo-generated electron-hole pair of the large area of the core-shell structure without any loss [37]. The above referred work indicates that the properties of CuO has been remarkably improved/modified when prepared by different techniques/systems/layers and no documents is there based on SiO_2@p-CuO photodetectors so far.

Hence, in this work, we have synthesized a core-shell SiO_2@p-CuO composite structure by the co-precipitation method. This core-shell SiO_2@p-CuO structure was used as a p-type layer for developing p-n junction diode on n-type Si to enhance their performance. The p- SiO_2@p-CuO/n-Si diode was inspected in dark and light surroundings using I-V characteristics. The important photo-diode parameters, namely ideality factor (n), barrier height (Φ_B), current of reverse saturation (I_o), photosensitivity (P_S), responsivity (R), external quantum efficiency (EQE %), and specific detectivity (D*) were estimated and interpreted.

2. Investigational method

2.1. Used materials

Copper nitrate ($Cu(NO_3)_2$, 95%, Nice), Ammonium hydroxide (NH_4OH, Merck life science), Tetraethyl orthosilicate (TEOS, ~98%, Sigma Aldrich), Ethanol, Acetic acid, and Triton x-100 were used as precursors for the synthesis of CuO and SiO_2@p-CuO

nanostructures. All chemicals used in this work were analytical reagent grade, which were utilized without any further purification.

2.2. Preparation of CuO nanoparticle

The co-precipitation method was adapted to synthesis the pure CuO nanoparticle using nitrate precursor. $Cu(NO_3)_2$ (0.2 moles) is added to 100 mL distilled water and stirred for 30 minutes to get a homogenous mixture. This aqueous solution was tuned to 9 pH using NH_4OH solution. The pH adjusted solution was heated to 90 ºC. The black in the colour precipitate was centrifuged by 3000 rpm and washed twice by distilled water to remove the supernatants.

2.3. Preparation of SiO_2 nanoparticle

The conventional Stober method was used to prepare spherical silica particles [38]. Precursors such as hexamethyldisiloxane (HMDSO), tetraethylorthosilicate (TEOS), tetramethylsilane (TMS), tetramethylorthosilicate (TMOS), and tetrapropylorthosilicate (TPOS) were used to synthesis SiO_2 spheres. Among them, TEOS precursor was one of the best precursors for SiO_2 synthesis due to potential formation of monodispersed and spherical particle by nominal catalysis rate under alkaline condition [39]. The hydrolysis and condensation of TEOS in low molecular weight alcohol with ammonia catalyst environment is favorable to synthesis monodispersed SiO_2 by monomer aggregation process with slow hydrolysis rate [40].

Analytical grade TEOS, anhydrous ethanol, and NH_4OH were used as a precursor for this synthesis. 1.2 mL of TOES was mixed within 10 ml of ethanol and stirred for 10 min under 400 rpm stirring. An appropriate amount of NH_4OH (0.75 mL) was diluted with 3 mL of water and was poured dropwise with former solution. Nonstop stirring for 2 h was done of the solution under ambient temperature. Then the synthesized spherical SiO_2 was centrifuged

and washed with ethanol two times to remove un-reactants. Separated SiO_2 particles were stored in ethanol-water (1:1) solvent for further use.

2.4. Preparation of core-shell SiO_2@p-CuO particles

The required amount of as-synthesized SiO_2 particles was dispersed in 100 mL distilled water under 400 rpm magnetic stirring. $Cu(NO_3)_2$ (200 mmole) was added to above the SiO_2 particles dispersed water solution. The solution pH was adjusted to 9 after the complete dissolution of $Cu(NO_3)_2$, and then the temperature of the solution was increased to 90 ºC for further initiation of co-precipitation. The final solution was washed with ethanol twice and annealed at 450 ºC.

2.5 . Device fabrication

The Silicon substrate (n-type) was used to construct the photosensitive device. The substrate was cleaned using piranha solution (H_2O_2+H_2SO_4) to remove the residual impurities on the substrate. SiO_2 oxide layer on the Si wafer was removed using diluted hydrofluoric acid. Annealed CuO and SiO_2@p-CuO were dispersed in cyclohexane+oleylamine solution and was drop cast over the n-Si substrate. Dried thin-film was annealed at 320 °C for one hour and silver past (ELTECK-corporation) was applied both-side of the diode to make better contact and it was dried at room temperature for 3 hours. The schematic illustration of core-shell SiO_2@p-CuO/n-Si diode is demonstrated in Fig. 1.

2.6 Characterization technique

The structural studies of as-synthesized and annealed CuO and SiO_2@p-CuO samples were performed by ‘X’PERT PAN analytical a powder X-ray diffraction diffractometer with CuK_α radiation of 1.5405 Å. Raman spectral analysis was studied through a HR 800 Raman spectrometer (Jobin Yvon) with 532 nm source of laser. The surface morphology was analysed by S-3400N Hitachi FE-SEM. The I-V characteristics of fabricated diodes were

performed through the Keithley source analyser (6517-B) equipped PEC-L01 portable solar simulator.

3. Results and discussion

3.1. Structural Studies

Acquired XRD reflection patterns of as-synthesized CuO and CuO annealed at 450 ℃, as-synthesized SiO_2@p-CuO, and SiO_2@p-CuO annealed at 450 ℃ were compared in Fig. 2. The as-synthesized CuO sample shows reflections corresponding to CuO along with a low intense $Cu(OH)_2$ peaks and was well matched with JCPDS card number 41-254 and 01-080-0656, respectively. Impurity, $Cu(OH)_2$ was disappeared after annealing and was displayed in CuO annealed at 450 ℃ in the Fig. 2. Observed XRD profiles of the pure CuO and CuO encapsulated SiO_2 nanoparticle indicating a monoclinic structure with C2/c space group. Moreover, better growth was seen for (111) plane in as-synthesized CuO. The preferential growth was changed into (002) plane after annealing at 450 ℃. Results indicate that the annealing temperature effectively modifies the growth of the CuO plane. In SiO_2@p-CuOcomposite, some of the peaks disappeared even annealed samples when compared to pure CuO, which suggests that the incorporation of the SiO_2 in the CuO system could affect the growth of the CuO planes.

3.2. Raman Spectral Analysis

The Raman spectrum of as-synthesized CuO, 450 ^oC annealed CuO, as-synthesized SiO_2@p-CuO, and 450 ^oC annealed SiO_2@p-CuO were shown in Fig. 3. The as-synthesized CuO exhibits three well-identified peaks, such as 294, 341, and 627 $cm^{-1,}$ which attributes the vibrations of A_g, B_g^1, and B_g^2, respectively [41]. Annealed CuO sample showed two well-identified peaks at 297 and 345 cm^{-1} and one low intense peak at 625 cm^{-1}. Three intense peaks at 302, 346 were observed for A_g and B_g^1 of CuO present in the as-synthesized SiO2@p-CuO core-shell nanoparticle and broad peak at 598 cm^{-1} may attribute the

combination of D_1 band of SiO_2 and B_g^2 band of CuO [42]. These intense peaks appeared for 450 ℃annealed SiO_2@p-CuOat 299,346, and597cm^{-1}.

3.3. Surface Morphology

Surface morphology of as-synthesized CuO annealed CuO, and SiO_2@p-CuOwere observed using FE-SEM analyzed, which are compared in Fig. 4. The surface morphology of CuO (Fig. 4 a, b, and c) illustrates that the derived particles appeared like dispersed thin cross-linked nanosheets. Observed nanosheets were in the thickness of ~140 nm in size. Morphology of as-synthesized SiO_2particles was monodispersed spherical shape particles, and the surface of the pure SiO_2 nanoparticle was smooth and uniform (Fig. 4 d, e, and f). The diameter of the as-synthesized SiO_2nanoparticle was in ~360 nm. The micrographs of SiO_2@p-CuO composite are also spherical particles with a rough surface; it is evident that the surface of the SiO_2 surface was covered with thin sheets of CuO. The distribution of CuO particles on SiO_2 was uniform, which confirmed the formation of SiO_2@p-CuO composite (Fig. 4 g, h, and i). Also, the diameter of the synthesized SiO_2@p-CuO is ~470 nm, and it is confirmed that the formed shell layer around 55 nm CuO on the SiO_2 surface.

3.4. I-V Characteristics

The electrical parameters of fabricated p-CuO/n-Si and SiO_2@p-CuO/n-Si diodes were estimated from I-V plots of bias voltage from voltage -3 to +3 and rectifying behaviour of the photodiode is shown in Fig. 5. The current conduction mechanism of above diodes were discussed based on thermionic emission theory using [43]:

$$I = I_0 \left[\exp\left(\frac{q(V-IR_s)}{nK_BT}\right) - 1\right] \qquad (1)$$

Where,

$$I_0 = AA^*T^2 \exp\left(-\frac{q\phi_B}{K_BT}\right) \qquad (2)$$

All used symbols are well-known [44, 45]. Calculated value of I_o for p-CuO/n-Si and SiO_2@p-CuO/n-Si diodes has been decreasing from 2.56×10^{-4} to 1.00×10^{-3} A and from

4.78×10^{-4} to 1.00×10^{-4} A, respectively in dark & light surroundings. The n and Φ_B of fabricated diode were calculated from following equation using intercepting of ln(J) vs. V plots (Fig. 6) [46],

$$n = \frac{q}{k_B T}\left(\frac{d(V)}{d(\ln(I))}\right) \quad (3)$$

$$\Phi_B = \frac{K_B T}{q} \ln\left(\frac{AA^* T^2}{I_0}\right) \quad (4)$$

Calculated value of n for p-CuO/n-Si and SiO_2@p-CuO/n-Si diodes were 6.04 and 3.96 respectively under light condition. Ideality factor n should be closer to one for attaining ideal behaviour of the device and the ideality factor of fabricated SiO_2@p-CuO/n-Si diode is closer to closer to one when compared to p-CuO/n-Si. Reduction of n value in illumination condition is due to the conversion proficiency of interface layer and lower barrier height. The values of Φ_B and n influenced by the native thin oxide layer and band edge, where the minority carriers reside near traps of carrier tunnelling and barrier inhomogeneities. Further to evaluate the performance of the photodiode the P_S, R, EQE %, and D* were calculated [47, 48]. The photosensitivity (P_S) is the relation between dark and photocurrent, which is calculated from the following relation,

$$P_s\ (\%) = \frac{I_{Ph} - I_D}{I_D} \times 100 \quad (5)$$

The photosensitivity of SiO_2@p-CuO/n-Si is several times higher than p-CuO/n-Si diode, which shown in Table 1. The P_s value for p-CuO/n-Si is noticed ~ 5320.3% while for SiO_2@p-CuO/n-Si is ~ 580471.4%, this shows about 110 times larger value. The photon generation in the layer large surface to volume ratio lead higher oxygen absorption that increases the photocurrent in the sensitive layer furthermore photo responsivity also increases. Another important parameter of photodetector is photo responsivity which help us to analyse the performance of the device and can be determine using [49, 50]:

$$R = \frac{I_{Ph}}{P \times A} \quad (6)$$

here, I_{ph} stand for photocurrent, p is irradiation, and A is the area of the power intensity of light on a sensitive layer. The optimized power intensity used in this work is 100 mW/cm^2. The photocurrent in the detector is varying on the intensity of light on the area of the sensitive layer. Fig. 7 (a) & (b) shows the comparison graph of photosensitivity, responsivity, quantum efficiency, and specific detectivity vs. voltage of p-CuO/n-Si and SiO_2@p-CuO/n-Si fabricated photodiode. The responsivity of the diode is varying with applied voltage, and it shows the responsivity increases with increasing the bias voltage. The R value for p-CuO/n-Si is estimated ~ 230.6 and for SiO_2@p-CuO/n-Si ~ 259.7 mA/W. The number of electrons detected due to the incident photon is EQE of diode, the coefficient of absorption of the sensitive layer and transfer efficiency of charge carries dominate the EQE, which is calculated from the following equation [51, 52]:

$$EQE = \frac{Rhc}{q\lambda} \quad (7)$$

The estimated EQE of p-CuO/n-Si is ~ 89.4 while it increases for SiO_2@p-CuO/n-Si and noticed ~ 100.7% may. The dark current is the main reason for the noise level in the device. The higher specific detectivity value implies that the ability to observe the signal from the noise environment that is given by the following relation [51, 52],

$$D^* = \frac{R \times A^{1/2}}{(2qI_D)^{1/2}} \quad (8)$$

The calculated D* value for SiO_2@p-CuO/n-Si is 1.715×10^{12} Jone, which is one order higher than p-CuO/n-Si diode viz. 1.561×10^{11}. These outcomes reveal that the fabricated SiO_2@p-CuO/n-Si photodiode is better to compare with p-CuO/n-Si. The photodetection properties of newly developed SiO_2@p-CuO/n-Si photodetector is comparable with previously reported CuO based photodetectors like; Zhang et al. reported the p-CuO/n-MoS_2 heterojunction based flexible photodetector developed via magnetron sputtering/CVD and noticed the detectivity of 3.27×10^8 Jones [18]. Hong et al. used solution process to develop CuO/Si nanowire like photodetector and investigated under different wavelengths and the

values of responsivity (R), and detectivity (D*) between 0.389 to 0.064 mA/W and 3×10^{9} to 7.6×10^{9} cm 0.040 to 0.123 A/W [19]. Fu et al. fabricated ZnO/CuO photodetector and noticed the values of P_s and R ~ 120 and 0.272 mA/W [20]. Noothongkaew et al. developed CuO/ZnO UV-photodetector and studied [21]. Also comparable to very recently documented CuO based photodetectors like; Yin et al. reported the development of photodetector based on CuO/Ni@CuO with high performance [22]. Tripathi et al. fabricated the tailored photodetector properties of CuO by tailoring the band gap through varying the morphology and noticed the P_s and D* of $\sim10^{3}$ and 2.24×10^{11} Jones at 900 nm and 122 and 2.74×10^{10} Jones at 250 nm light wavelengths and the UV-C detector indicates a P_s of 1.8 and D* of 4×10^{9} Jones at 250 nm light wavelength [23]. Ji et al. fabricated the p-CuO nanospheres/n-ZnO nanorods UV-photodetector [24]. From above results and comparison with earlier reported values on CuO based photodetectors, the currently developed SiO_2@p-CuO/n-Si photodiode/photodetector will be highly applicable in photodetection with high efficiency.

4. Conclusion

Composite SiO_2@p-CuO nanostructure was fabricated through co-precipitation route with micro-emulsion synthesized SiO_2 spheres. The diffraction pattern result reveals that the formation of single-phase monoclinic CuO in the pure and core-shell composite structure. Improvement in phase purity of CuO at high-temperature calcined samples was confirmed with Raman analysis. The FE-SEM results show the Formation of CuO layers on SiO_2 spheres as a core-shell. The diode parameters were studied from I-V characteristics. The P_s value for p-CuO/n-Si and SiO_2@p-CuO/n-Si diodes is estimated ~ 5320.3% and ~ 580471.4%, respectively, this shows about 110 times larger value for SiO_2@p-CuO/n-Si diodes. The R value for p-CuO/n-Si and SiO_2@p-CuO/n-Si diodes is estimated ~ 230.6 and ~ 259.7 mA/W, indicates then enhancement. The estimated EQE of p-CuO/n-Si and is ~ 89.4 while it increases for SiO_2@p-CuO/n-Si and noticed ~ 100.7%. The calculated D* value for

SiO_2@p-CuO/n-Si is 1.715×10^{12} Jone, which is one order higher than p-CuO/n-Si diode viz. 1.561×10^{11}. The obtained outcomes recommend the developed structure of SiO_2@p-CuO/n-Si diode possess remarkably improved photodetection properties hence it is a potential candidate for photo-detector application.

Acknowledgement

The Author (D. Thangaraju) sincerely thanks Science and Engineering Research Board (ECR/2017/002974), Department of Science and Technology, Government of India, for the financial support. This research was funded by the Deanship of Scientific Research at Princess Nourah bint Abdulrahman University through the Fast-track Research Funding Program. The author (A. Durairajan) thanks the PFST for project under UI D/CTM/50025/2019, COM-PETE 2020 Programme and FCT Post-Doctoral grant No. BPD/UI96/ 7799/2019; 50025: I3N.

Declaration of Competing Interest

The authors declared that there is no conflict of interest.

Credit author statement

All the authors are contributing equally in preparation of the manuscript

Reference

[1] Z. Li, H. Li, Z. Wu, M. Wang, J. Luo, H. Torun, et al., Advances in designs and mechanisms of semiconducting metal oxide nanostructures for high-precision gas sensors operated at room temperature, Materials Horizons, 6(2019) 470-506.
[2] E. Fortunato, P. Barquinha, R. Martins, Oxide semiconductor thin-film transistors: a review of recent advances, Advanced Materials, 24(2012) 2945-86.
[3] Q. Hong, Y. Cao, J. Xu, H. Lu, J. He, J.-L. Sun, Self-powered ultrafast broadband photodetector based on p–n heterojunctions of CuO/Si nanowire array, ACS applied materials & interfaces, 6(2014) 20887-94.
[4] A.V. Singh, M.H.D. Ansari, D. Rosenkranz, R.S. Maharjan, F.L. Kriegel, K. Gandhi, et al., Artificial Intelligence and Machine Learning in Computational Nanotoxicology: Unlocking and Empowering Nanomedicine, Advanced Healthcare Materials, 1901862.
[5] A.V. Singh, Biotechnological applications of supersonic cluster beam-deposited nanostructured thin films: Bottom-up engineering to optimize cell–protein–surface interactions, Journal of biomedical materials research Part A, 101(2013) 2994-3008.
[6] Z. Zheng, L. Gan, H. Li, Y. Ma, Y. Bando, D. Golberg, et al., A fully transparent and flexible ultraviolet–visible photodetector based on controlled electrospun ZnO-CdO heterojunction nanofiber arrays, Advanced Functional Materials, 25(2015) 5885-94.
[7] N.M. Abd-Alghafour, N.M. Ahmed, Z. Hassan, Fabrication and characterization of V2O5 nanorods based metal–semiconductor–metal photodetector, Sensors and Actuators A: Physical, 250(2016) 250-7.
[8] P. Wang, X. Zhao, B. Li, ZnO-coated CuO nanowire arrays: fabrications, optoelectronic properties, and photovoltaic applications, Optics Express, 19(2011) 11271-9.
[9] A. V Singh, R. Patil, A. Anand, P. Milani, W. Gade, Biological synthesis of copper oxide nano particles using Escherichia coli, Current Nanoscience, 6(2010) 365-9.
[10] K. Mageshwari, R. Sathyamoorthy, Physical properties of nanocrystalline CuO thin films prepared by the SILAR method, Materials Science in Semiconductor Processing, 16(2013) 337-43.
[11] F.A. Akgul, G. Akgul, N. Yildirim, H.E. Unalan, R. Turan, Influence of thermal annealing on microstructural, morphological, optical properties and surface electronic structure of copper oxide thin films, Materials Chemistry and Physics, 147(2014) 987-95.
[12] A. Ghosh, M. Mitra, D. Banerjee, A. Mondal, Facile electrochemical deposition of Cu7Te4 thin films with visible-light driven photocatalytic activity and thermoelectric performance, RSC Advances, 6(2016) 22803-11.
[13] A. Rydosz, A. Szkudlarek, Gas-sensing performance of M-doped CuO-based thin films working at different temperatures upon exposure to propane, Sensors, 15(2015) 20069-85.
[14] S. Anandan, X. Wen, S. Yang, Room temperature growth of CuO nanorod arrays on copper and their application as a cathode in dye-sensitized solar cells, Materials Chemistry and Physics, 93(2005) 35-40.
[15] R.R. Prabhu, A.C. Saritha, M.R. Shijeesh, M.K. Jayaraj, Fabrication of p-CuO/n-ZnO heterojunction diode via sol-gel spin coating technique, Materials Science and Engineering: B, 220(2017) 82-90.
[16] A. Tombak, M. Benhaliliba, Y.S. Ocak, T. Kiliçoglu, The novel transparent sputtered p-type CuO thin films and Ag/p-CuO/n-Si Schottky diode applications, Results in Physics, 5(2015) 314-21.
[17] S. Annathurai, S. Chidambaram, B. Baskaran, G.K.D. Prasanna Venkatesan, Green Synthesis and Electrical Properties of p-CuO/n-ZnO Heterojunction Diodes, Journal of Inorganic and Organometallic Polymers and Materials, 29(2019) 535-40.
[18] K. Zhang, M. Peng, W. Wu, J. Guo, G. Gao, Y. Liu, et al., A flexible p-CuO/n-MoS2 heterojunction photodetector with enhanced photoresponse by the piezo-phototronic effect, Materials Horizons, 4(2017) 274-80.

[19] S. Wang, C. Hsiao, S. Chang, Z.Y. Jiao, S. Young, S. Hung, et al., ZnO Branched Nanowires and the p-CuO/n-ZnO Heterojunction Nanostructured Photodetector, IEEE Transactions on Nanotechnology, 12(2013) 263-9.
[20] Q.-M. Fu, D.-C. He, Z.-C. Yao, J.-L. Peng, H.-Y. Zhao, H. Tao, et al., Self-powered ultraviolet photodetector based on ZnO nanorod arrays decorated with sea anemone-like CuO nanostructures, Materials Letters, 222(2018) 74-7.
[21] S. Noothongkaew, O. Thumthan, K.-S. An, UV-Photodetectors based on CuO/ZnO nanocomposites, Materials Letters, 233(2018) 318-23.
[22] W. Yin, J. Yang, K. Zhao, A. Cui, J. Zhou, W. Tian, et al., High Responsivity and External Quantum Efficiency Photodetectors Based on Solution-Processed Ni-Doped CuO Films, ACS Applied Materials & Interfaces, 12(2020) 11797-805.
[23] A. Tripathi, T. Dixit, J. Agrawal, V. Singh, Bandgap engineering in CuO nanostructures: Dual-band, broadband, and UV-C photodetectors, Applied Physics Letters, 116(2020) 111102.
[24] Y. Ji, U. Jung, Z. Xian, D. Kim, J. Yu, J. Park, Ultraviolet photodetectors using hollow p-CuO nanospheres/n-ZnO nanorods with a pn junction structure, Sensors and Actuators A: Physical, 304(2020) 111876.
[25] P. Kasian, S. Pukird, Gas Sensing Properties of CuO Nanostructures Synthesized by Thermal Evaporation of Copper Metal Plate, Advanced Materials Research, 93-94(2010) 316-9.
[26] K.C. Sanal, L.S. Vikas, M.K. Jayaraj, Room temperature deposited transparent p-channel CuO thin film transistors, Applied Surface Science, 297(2014) 153-7.
[27] H. Faiz, K. Siraj, M.F. Khan, M. Irshad, S. Majeed, M.S. Rafique, et al., Microstructural and optical properties of dysprosium doped copper oxide thin films fabricated by pulsed laser deposition technique, Journal of Materials Science: Materials in Electronics, 27(2016) 8197-205.
[28] J. Zheng, W. Zhang, Z. Lin, C. Wei, W. Yang, P. Dong, et al., Microwave synthesis of 3D rambutan-like CuO and CuO/reduced graphene oxide modified electrodes for non-enzymatic glucose detection, Journal of Materials Chemistry B, 4(2016) 1247-53.
[29] M. Lamri Zeggar, L. Chabane, M.S. Aida, N. Attaf, N. Zebbar, Solution flow rate influence on properties of copper oxide thin films deposited by ultrasonic spray pyrolysis, Materials Science in Semiconductor Processing, 30(2015) 645-50.
[30] A.V. Singh, S. Baylan, B.-W. Park, G. Richter, M. Sitti, Hydrophobic pinning with copper nanowhiskers leads to bactericidal properties, PloS one, 12(2017) e0175428.
[31] P. Venkateswari, P. Thirunavukkarasu, M. Ramamurthy, M. Balaji, J. Chandrasekaran, Optimization and characterization of CuO thin films for P–N junction diode application by JNSP technique, Optik, 140(2017) 476-84.
[32] A. Chen, H. Long, X. Li, Y. Li, G. Yang, P. Lu, Controlled growth and characteristics of single-phase Cu2O and CuO films by pulsed laser deposition, Vacuum, 83(2009) 927-30.
[33] T. Maruyama, Copper oxide thin films prepared by chemical vapor deposition from copper dipivaloylmethanate, Solar Energy Materials and Solar Cells, 56(1998) 85-92.
[34] A.W. Weimer, Particle atomic layer deposition, Journal of Nanoparticle Research, 21(2019) 9.
[35] R.M. Pallares, K.P. Carter, S.E. Zeltmann, T. Tratnjek, A.M. Minor, R.J. Abergel, Selective Lanthanide Sensing with Gold Nanoparticles and Hydroxypyridinone Chelators, Inorganic chemistry, 59(2020) 2030-6.
[36] X. Wang, W. Tian, M. Liao, Y. Bando, D. Golberg, Recent advances in solution-processed inorganic nanofilm photodetectors, Chemical Society Reviews, 43(2014) 1400-22.
[37] D. Thangaraju, R. Marnadu, V. Santhana, A. Durairajan, P. Kathirvel, J. Chandrasekaran, et al., Solvent influenced synthesis of single-phase SnS 2 nanosheets for solution-processed photodiode fabrication, CrystEngComm, 22(2020) 525-33.
[38] D. Thangaraju, A. Durairajan, D. Balaji, S. Moorthy Babu, Y. Hayakawa, SiO2/KGd(WO4)2:Eu3+ composite luminescent nanoparticles: Synthesis and characterization, Materials Chemistry and Physics, 135(2012) 1115-21.

[39] K.D. Kim, H.T. Kim, Formation of Silica Nanoparticles by Hydrolysis of TEOS Using a Mixed Semi-Batch/Batch Method, Journal of Sol-Gel Science and Technology, 25(2002) 183-9.
[40] K. Cho, H. Chang, D.S. Kil, J. Park, H.D. Jang, H.Y. Sohn, Mechanisms of the formation of silica particles from precursors with different volatilities by flame spray pyrolysis, Aerosol Science and Technology, 43(2009) 911-20.
[41] B.J. Rani, G. Ravi, R. Yuvakkumar, Z.M. Hasan, S. Ravichandran, S.I. Hong, Binder free, robust and scalable CuO@GCE modified electrodes for efficient electrochemical water oxidation, Materials Chemistry and Physics, 239(2020) 122321.
[42] S.T. Hossain, Y. Almesned, K. Zhang, E.T. Zell, D.T. Bernard, S. Balaz, et al., Support structure effect on CO oxidation: A comparative study on SiO2 nanospheres and CeO2 nanorods supported CuOx catalysts, Applied Surface Science, 428(2018) 598-608.
[43] V. Balasubramani, J. Chandrasekaran, R. Marnadu, P. Vivek, S. Maruthamuthu, S. Rajesh, Impact of Annealing Temperature on Spin Coated V2O5 Thin Films as Interfacial Layer in Cu/V2O5/n-Si Structured Schottky Barrier Diodes, Journal of Inorganic and Organometallic Polymers and Materials, 29(2019) 1533-47.
[44] A. Buyukbas-Uluşan, S.A. Yerişkin, A. Tataroğlu, M. Balbaşı, Y.A. Kalandaragh, Electrical and impedance properties of MPS structure based on (Cu 2 O–CuO–PVA) interfacial layer, Journal of Materials Science: Materials in Electronics, 29(2018) 8234-43.
[45] A.B. Uluşan, A. Tataroğlu, Y. Azizian-Kalandaragh, Ş. Altındal, On the conduction mechanisms of Au/(Cu 2 O–CuO–PVA)/n-Si (MPS) Schottky barrier diodes (SBDs) using current–voltage–temperature (I–V–T) characteristics, Journal of Materials Science: Materials in Electronics, 29(2018) 159-70.
[46] R. Marnadu, J. Chandrasekaran, M. Raja, M. Balaji, S. Maruthamuthu, P. Balraju, Influence of metal work function and incorporation of Sr atom on WO3 thin films for MIS and MIM structured SBDs, Superlattices and Microstructures, 119(2018) 134-49.
[47] G. Liu, Z. Li, X. Chen, W. Zheng, W. Feng, M. Dai, et al., Non-planar vertical photodetectors based on free standing two-dimensional SnS 2 nanosheets, Nanoscale, 9(2017) 9167-74.
[48] M. Shkir, I. Ashraf, K.V. Chandekar, I. Yahia, A. Khan, H. Algarni, et al., A significant enhancement in visible-light photodetection properties of chemical spray pyrolysis fabricated CdS thin films by novel Eu doping concentrations, Sensors and Actuators A: Physical, 301(2020) 111749.
[49] M. Shkir, I. Ashraf, S. AlFaify, A.M. El-Toni, M. Ahmed, A. Khan, A noticeable effect of Pr doping on key optoelectrical properties of CdS thin films prepared using spray pyrolysis technique for high-performance photodetector applications, Ceramics International, 46(2020) 4652-63.
[50] M. Shkir, I.M. Ashraf, A. Khan, M.T. Khan, A.M. El-Toni, S. AlFaify, A facile spray pyrolysis fabrication of Sm:CdS thin films for high-performance photodetector applications, Sensors and Actuators A: Physical, 306(2020) 111952.
[51] I.M. Ashraf, M. Shkir, S. AlFaify, F. Abdel-Wahab, A.M. Ali, M.A. Sebak, et al., Development and characterization of TlGaSe2 thin film-based photodetector for visible-light photodetector applications, Optical Materials, 103(2020) 109834.
[52] S. Mohd, I.M. Ashraf, S. AlFaify, Surface area, optical and electrical studies on PbS nanosheets for visible light photo-detector application, Physica Scripta, 94(2019) 025801.

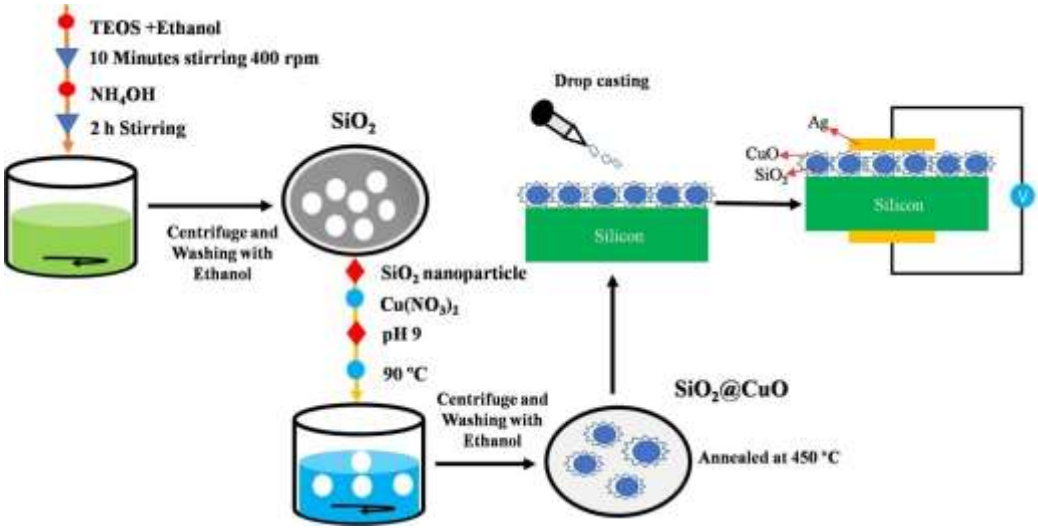

Fig. 1. Schematic diagram of synthesis of SiO_2@p-CuO and fabricated SiO_2@p-CuO/n-Si junction diode.

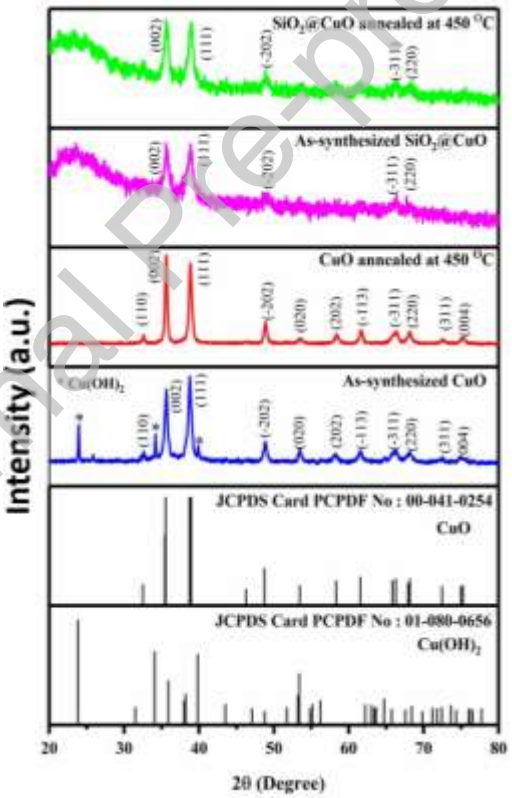

Fig. 2. Comparative XRD patterns of as-synthesized, 450 ^oC annealed CuO, as-synthesized, and 450 ^oC annealed SiO_2@CuO.

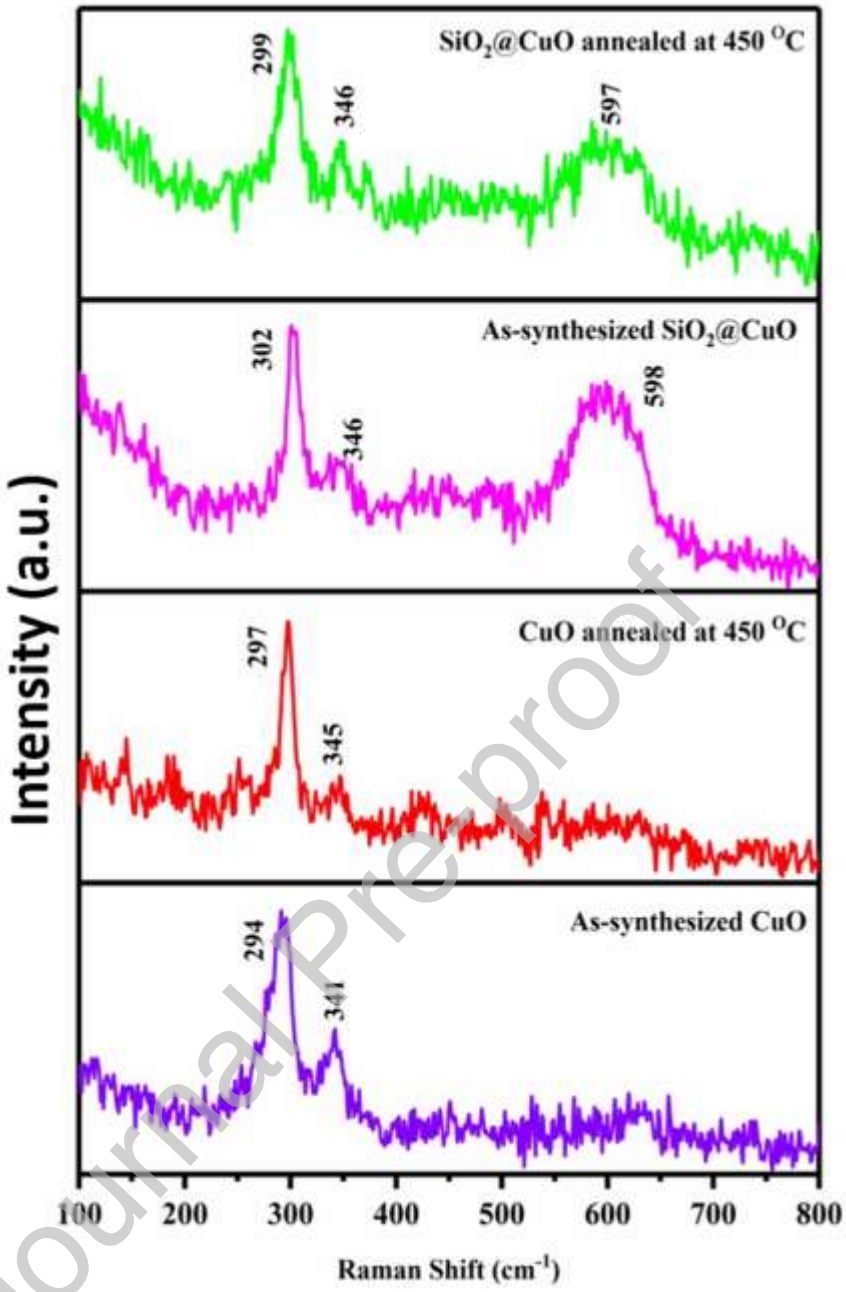

Fig. 3. Comparative Raman spectra of as-synthesized, 450 ^{o}C annealed CuO, as-synthesized, and 450 ^{o}C annealed SiO_2@CuO.

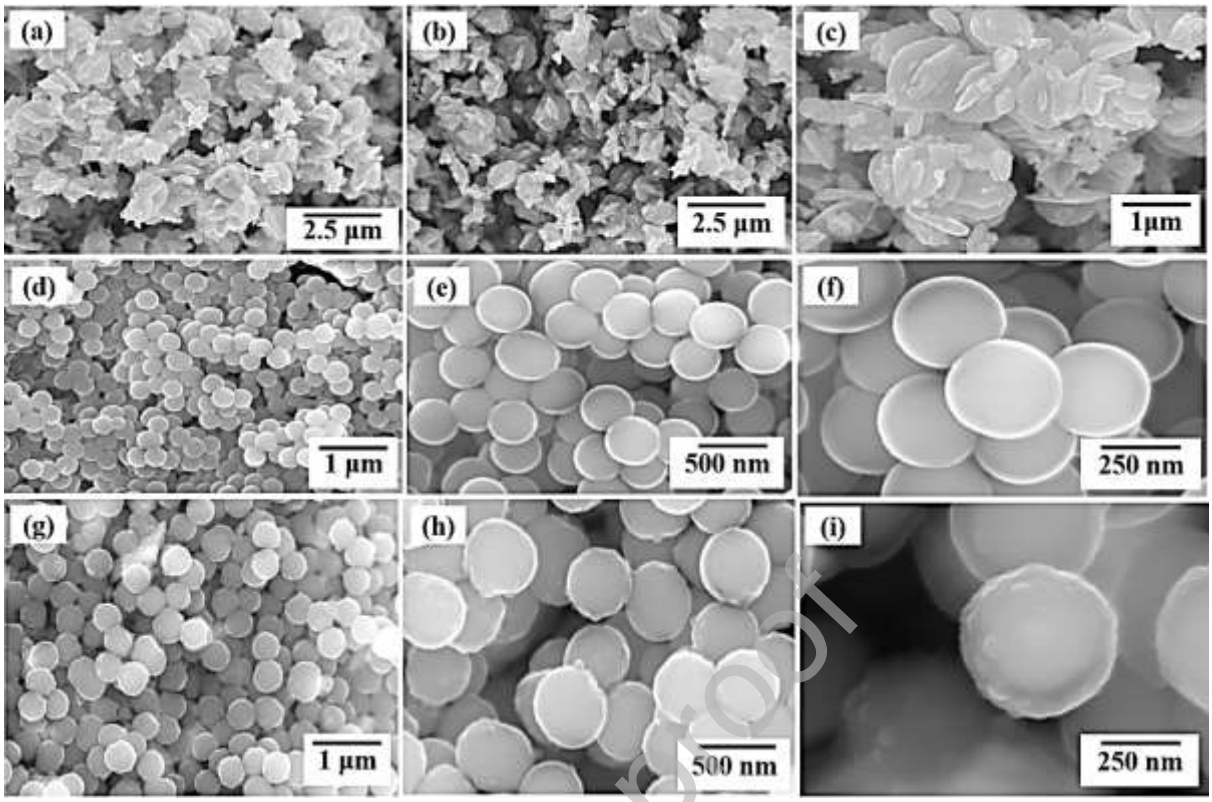

Fig. 4. SEM Micrographs of 450 ^{o}C annealed CuO (a-c), as synthesized SiO_2 (d-f) and 450 ^{o}C annealed SiO_2@p-CuO (g-i).

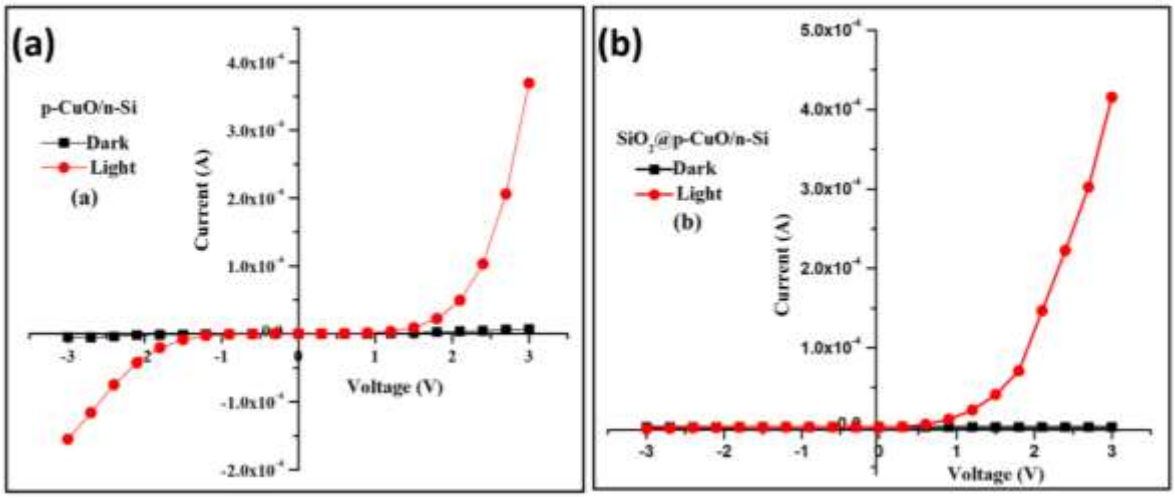

Fig. 5. I–V characteristics of p-CuO/n-Si (a) and SiO_2@p-CuO/n-Si (b) fabricated photodiode.

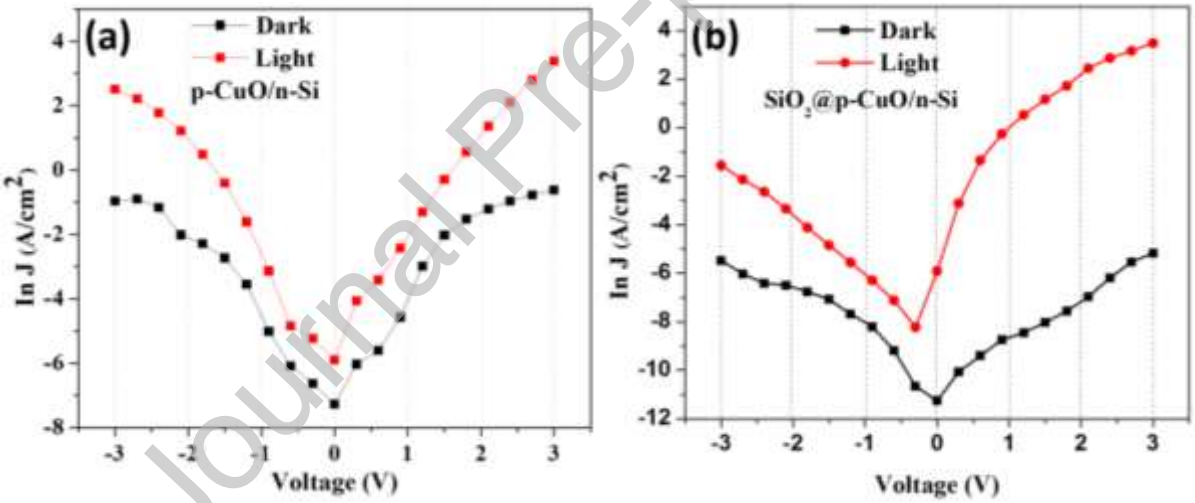

Fig. 6. Semi-logarithmic plot of ln (J) vs. V for p-CuO/n-Si (a) and SiO_2@p-CuO/n-Si (b)fabricated photodiode.

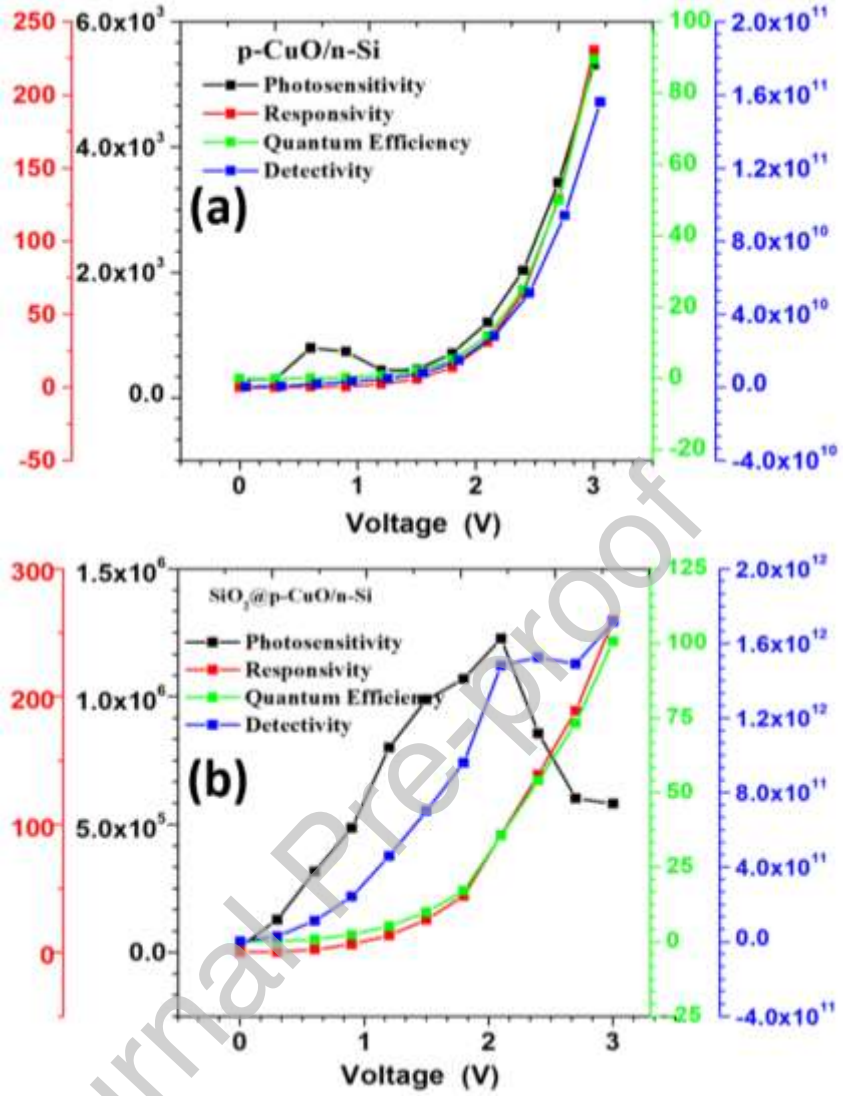

Fig. 7. Comparison of photosensitivity, responsivity, quantum efficiency, and specific detectivity vs. Voltage graph of p-CuO/n-Si (a) and SiO_2@p-CuO/n-Si (b) fabricated photodiode.

Table 1. Photodiode parameter n, Φ_B, I_o, P_S, R, QE%, and D* of p-CuO/n-Si and SiO_2@p-CuO/n-Si fabricated photodiode.

Diode	n		Φ_B (eV)		I_o (A)		P_S (%)	R (mA/W)	QE (%)	D ($\times 10^9$) (Jone)
	Dark	Light	Dark	Light	Dark	Light				
p-CuO/n-Si	9.57	6.04	0.669	0.634	2.56×10^{-4}	1.00×10^{-3}	5320.3	230.6	89.4	1.561×10^{11}
SiO_2@p-CuO/ n-Si	8.84	3.96	0.773	0.694	4.78×10^{-6}	1.00×10^{-4}	580471.4	259.7	100.7	1.715×10^{12}